

## Shape Fluctuations of Polymerized or Solidlike Membranes

Reinhard Lipowsky<sup>(a)</sup> and Marc Girardet

*Sektion Physik der Universität München, Theresienstrasse 37, 8000 München, Germany*

(Received 2 July 1990)

Polymerized membranes or solidlike elastic sheets are studied by scaling arguments and Monte Carlo simulations. We find that the roughness exponent  $\zeta$  has the value  $\zeta = \frac{1}{2}$  while previous simulations gave  $\zeta = 0.64 \pm 0.04$ . Our data are consistent with a *finite* value of the shear modulus on large scales. We also find a pronounced *crossover* from fluidlike behavior with  $\zeta = 1$  on small scales to solidlike behavior with  $\zeta = \frac{1}{2}$  on large scales. This crossover should be observable in experiments on the flickering of red blood cells.

PACS numbers: 64.60.Fr, 05.40.+j, 82.70.-y

Polymerized membranes are two-dimensional sheets of molecules with a fixed connectivity such as, e.g., protein networks of biological membranes or bilayers of polymerized lipids.<sup>1,2</sup> Recently, a substantial amount of *theoretical* work has been devoted to such membranes.<sup>3-12</sup> First, self-intersecting "phantom" membranes have been studied which can exhibit crumpled states.<sup>3</sup> Real membranes cannot self-intersect, however, and this constraint of self-avoidance *prevents* crumpling at all temperatures.<sup>4-6</sup>

The uncrumpled state of a polymerized membrane still exhibits interesting scaling properties: For a membrane segment of linear size  $L$ , the transverse displacements have a typical amplitude  $L_{\perp} \sim L^{\zeta}$  governed by the roughness exponent  $\zeta$ . One may then introduce a scale-dependent bending rigidity which grows as  $\sim L^{\eta_{\kappa}}$ , with  $\eta_{\kappa} = 2 - 2\zeta$ .<sup>7,8</sup> Likewise, the shear modulus behaves as  $\sim L^{-\eta_{\mu}}$ , with  $\eta_{\mu} = 4\zeta - 2$ .<sup>9</sup>

Recently, Monte Carlo (MC) and molecular-dynamics simulations have been performed in order to determine the value of  $\zeta$ . In these simulations, a triangular network of "balls" connected by "tethers" was studied which gave the value  $\zeta = 0.64 \pm 0.04$ .<sup>10-12</sup> Here, we also report results of MC simulations but for the continuum model of a solidlike elastic sheet.<sup>7,13</sup> The latter approach has been previously applied to fluid membranes.<sup>14</sup>

Our results are as follows. First, scaling arguments give (i) the lower bound  $\zeta \geq \frac{1}{2}$  for the roughness exponent, and (ii) the value  $\zeta = \frac{1}{2}$  for *zero* bending rigidity,  $\kappa = 0$ , provided the model is well defined in this limit. We then present extensive MC simulations which reveal that the limiting value  $\zeta = \frac{1}{2}$  applies, in fact, to polymerized membranes for *general*  $\kappa \geq 0$ . Obviously, this value is very different from the values  $\zeta = 0.64 \pm 0.04$  obtained for tethered networks.<sup>10-12</sup> We show that this discrepancy arises from a pronounced *crossover*: For relatively large bending rigidity or relatively small shear modulus, the small-scale excitations of the membrane are characterized by  $\zeta = 1$  as for fluid membranes,<sup>15,16</sup> and one has to probe undulations beyond a certain crossover scale in order to see the true asymptotic behavior with  $\zeta = \frac{1}{2}$ . Thus, the values for  $\zeta$  obtained from previous simula-

tions of tethered networks represent *effective* exponents which reflect this crossover.

Our results have important consequences: (i) The partial resummation of perturbation theory performed by Nelson and Peliti<sup>7</sup> gives, in fact, the correct value of  $\zeta$ . This is quite unexpected. (ii) The value  $\zeta = \frac{1}{2}$  implies that the critical exponent  $\eta_{\mu}$  for the shear modulus is zero since  $\eta_{\mu} = 4\zeta - 2$  as mentioned. In such a case, the shear modulus could still vanish with a weak logarithmic scale dependence. However, our data do not give any indication of such a logarithmic behavior and thus are consistent with a *finite* value of the shear modulus on large scales. (iii) We estimate that the crossover between fluidlike and solidlike behavior can be studied in experiments on the flickering of red blood cells,<sup>17,18</sup> see (15) below. (iv) Unbinding transitions of polymerized membranes interacting with nonretarded van der Waals interactions belong to the intermediate fluctuation regime with rather complex critical behavior.<sup>8</sup>

On length scales which are large compared to the mesh size of the polymerized network, the membrane can be viewed as a thin solidlike elastic sheet. Its configurations are then described by two lateral displacement fields,  $u_1$  and  $u_2$ , and a transverse displacement field,  $l$ , which depend on the coordinate,  $\mathbf{x} = (x_1, x_2)$ , of a planar reference state. The strain tensor  $u_{ij}$  is then given by<sup>13</sup>

$$u_{ij} = \frac{1}{2} [\partial_j u_i + \partial_i u_j + \partial_i l \partial_j l], \quad (1)$$

with  $\partial_i \equiv \partial/\partial x_i$  and  $i, j = 1, 2$ , and the elastic energy has the form

$$\mathcal{H}_e\{l, u_1, u_2\} = \int d^2x \left\{ \frac{1}{2} \kappa (\nabla^2 l)^2 + \frac{1}{2} K_A (u_{11} + u_{22})^2 + \mu \left[ \frac{1}{2} (u_{11} - u_{22})^2 + 2u_{12}^2 \right] \right\}, \quad (2)$$

where  $\kappa$ ,  $K_A$ , and  $\mu$  are the bending rigidity, modulus of area compressibility, and shear modulus, respectively. In addition, we include an external potential  $V(l)$  which confines the shape fluctuations of the membrane. Thus, we consider the effective Hamiltonian

$$\mathcal{H}\{l, u_1, u_2\} = \mathcal{H}_e\{l, u_1, u_2\} + \int d^2x V(l(x)) \quad (3)$$

for the membrane displacements, where a small-scale cutoff  $a$  is implicitly contained. One may now perform the partial trace over the phononlike fields,  $u_1$  and  $u_2$ , and obtain an effective Hamiltonian for  $l$  alone which depends on  $\mu$  and  $K_A$  only through the two-dimensional Young modulus,<sup>7</sup>

$$Y \equiv 4\mu K_A / (\mu + K_A). \quad (4)$$

In the absence of an external potential, i.e., for  $V(l) \equiv 0$ , the roughness of the membrane can be characterized by the difference correlation function

$$\Delta C(x) \equiv \frac{1}{2} \langle [l(\mathbf{x}) - l(\mathbf{0})]^2 \rangle, \quad (5)$$

with<sup>8</sup>

$$\Delta C(x) \approx \mathcal{A}^2 x^{2\zeta} \text{ for large } x. \quad (6)$$

In general, the roughness exponent  $\zeta$  satisfies  $0 \leq \zeta \leq 1$ . For  $Y > 0$ , the amplitude  $\mathcal{A} = \mathcal{A}_{s_0}$  can be determined by the following scaling argument. First, introduce the rescaled variable  $\bar{l} \equiv (\kappa/T)^{1/2} l$ . The Boltzmann factor for  $\bar{l}$  depends, apart from the small-scale cutoff  $a$ , only on the rescaled Young modulus  $\bar{Y} \equiv YT/\kappa^2$  which has the dimension of  $(\text{length})^{-2}$ . Quite generally, the amplitude  $\mathcal{A}$  in (6) should not depend on the small-scale cutoff.<sup>8</sup> It then follows from dimensional analysis that this amplitude is given by

$$\mathcal{A}_{s_0}^2 = \mathcal{D}_{s_0} (\kappa/Y) \bar{Y}^\zeta = \mathcal{D}_{s_0} T^\zeta / \kappa^{2\zeta - 1} Y^{1-\zeta}, \quad (7)$$

where  $\mathcal{D}_{s_0}$  is a dimensionless coefficient. Obviously, the roughness must decrease with increasing  $\kappa$ . It then follows from (7) that  $\zeta \geq \frac{1}{2}$ . Furthermore, if  $\mathcal{A}$  is finite for  $\kappa=0$ , the expression in (7) implies  $\zeta = \frac{1}{2}$  in this limit.

For  $\bar{Y}=0$ , the model as given by (2) describes an uncrumpled fluid membrane with  $\zeta=1$  and  $\mathcal{A} = \mathcal{A}_\eta \sim (T/\kappa)^{1/2}$ . For finite but *small*  $\bar{Y}$ , the fluctuations are still fluidlike on small scales but become solidlike on sufficiently large scales. This crossover is described by

$$\Delta C(x) \approx (\kappa/Y) \mathcal{D} (T^{1/2} Y^{1/2} x / \kappa), \quad (8)$$

with  $\mathcal{D}(t) \approx \mathcal{D}_{s_0} t^{2\zeta}$  for large  $t$  and  $\mathcal{D}(t) \approx \mathcal{D}_\eta t^2$  for small  $t$ .

Next, consider the shape fluctuations of the polymerized membrane when confined by the external potential

$$V(l) = \begin{cases} \infty & \text{for } l \leq 0, \\ Pl & \text{for } l > 0, \end{cases} \quad (9)$$

with a hard wall at  $l=0$ . For external pressure,  $P > 0$ , the membrane has a finite separation  $\langle l \rangle$  from the wall. As  $P$  goes to zero, the membrane unbinds from the wall and<sup>8,14,16</sup>

$$\langle l \rangle \sim 1/P^\psi \text{ with } \psi = \zeta / (2 + \zeta). \quad (10)$$

Now, the scaling arguments described above lead to the

scaling form

$$\langle l \rangle \approx (\kappa/Y)^{1/2} \mathcal{Z} (P \kappa^{5/2} / T^2 Y^{3/2}), \quad (11)$$

with  $\mathcal{Z}(p) \approx \mathcal{Z}_{s_0} / p^\psi$  for small  $p$  and  $\mathcal{Z}(p) \approx \mathcal{Z}_\eta / p^{1/3}$  for large  $p$ .

In the MC work, the spatial coordinate  $\mathbf{x}$  is replaced by a square lattice with lattice constant  $a$ . The membrane configuration is then specified by the dimensionless displacement fields  $z \equiv l/l_{sc}$  and  $y_i \equiv u_i/u_{sc}$ , where  $l_{sc}$  and  $u_{sc}$  are two scale factors. It is convenient to choose  $u_{sc}/a \equiv (l_{sc}/a)^2$  and  $l_{sc} \equiv a$ , which leads to

$$u_{ij} \approx y_{ij} \equiv \frac{1}{2} [\tilde{\partial}_i y_j + \tilde{\partial}_i y_j + \tilde{\partial}_i z \tilde{\partial}_j z], \quad (12)$$

where  $\tilde{\partial}_i$  represents a suitable discretization of  $\partial/\partial x_i$ . The discretized effective Hamiltonian  $\mathcal{H}\{z, y_1, y_2\}/T$  as obtained from (3) and (9) then depends on the dimensionless parameters  $\kappa_0 \equiv \kappa/T$ ,  $K_{A0} \equiv K_A a^2/T$ ,  $\mu_0 \equiv \mu a^2/T$ , and  $P_0 \equiv P a^3/T$ . Likewise, the rescaled Young modulus is given by  $Y_0 \equiv 4\mu_0 K_{A0} / (\mu_0 + K_{A0}) = Y a^2/T$ . This discretized model has been studied for periodic boundary conditions using a vectorized MC code which is an extension of the code in Ref. 14. This code now performs up to 180 megaflops per processor on a Cray Y-MP computer.

The results of our simulations are presented in Figs. 1-3 and in Table I. In Fig. 1, the behaviors of  $\langle z \rangle$  and  $\xi_\perp \equiv ((z - \langle z \rangle)^2)^{1/2}$  are shown as a function of pressure  $P_0$  (i) for  $\kappa_0=0$  and (ii) for two small but finite values of  $\kappa_0$ . Inspection of Fig. 1 shows that the limit of zero  $\kappa$  is not singular. Furthermore, the data for  $\langle z \rangle$  lead to  $\psi = \frac{1}{5}$  and thus to  $\zeta = 2\psi / (1 - \psi) = 1/2$  in agreement with the scaling arguments.

The range of  $P_0$  values displayed in Fig. 1 is limited to about three decades by finite-size effects and critical slowing down.<sup>19</sup> A much larger range can be studied, however, for the reduced pressure

$$p \equiv P \kappa^{5/2} / T^2 Y^{3/2} = P_0 \kappa_0^{5/2} / Y_0^{3/2}, \quad (13)$$

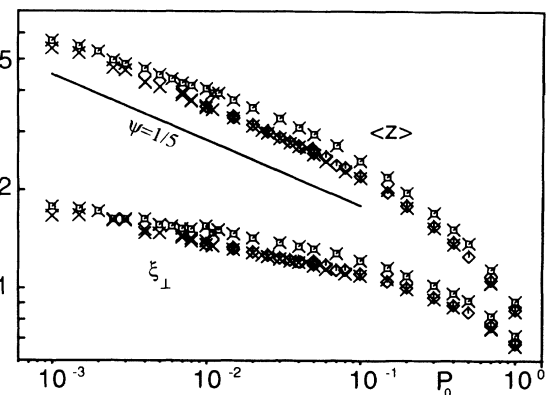


FIG. 1. Membrane separation  $\langle z \rangle$  and roughness  $\xi_\perp$  as a function of external pressure  $P_0$  for  $\kappa_0=0$  and for two small but finite values of  $\kappa_0$ ; compare Table I. The straight line has slope  $-\frac{1}{5}$ .

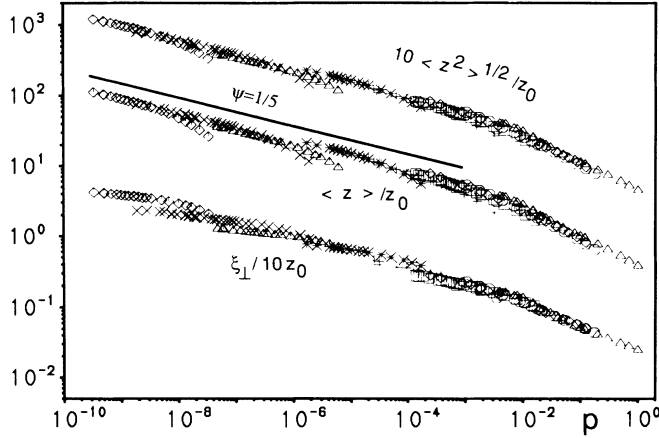


FIG. 2. Rescaled separation  $\langle z \rangle / z_0$  with  $z_0 = (\kappa_0 / Y_0)^{1/2}$  as a function of rescaled pressure  $p = P_0 \kappa_0^{3/2} / Y_0^{3/2}$ . The symbols are explained in Table I. The straight line has slope  $-\frac{1}{5}$ .

which determines the shape function  $Z(p)$  in (11). As shown in Fig. 2 and Table I, our data for different combinations of  $\kappa_0$ ,  $K_{A0}$ , and  $\mu_0$  extend over *ten decades* in the reduced pressure  $p$ . The entries in Table I are ordered according to the size of  $z_0 \equiv (\kappa_0 / Y_0)^{1/2}$ : Smaller and larger values of  $z_0$  correspond to a range of smaller and larger  $p$  values in Fig. 2, respectively. The tethered networks studied previously are characterized by<sup>3</sup>  $Y_0 \approx 20$  and  $\kappa_0 \geq 0.46$  which belongs to an intermediate value of  $z_0$  and, thus, to a  $p$  range within the crossover region. Our data do not indicate any confluent logarithmic singularities for this critical behavior; they are therefore consistent with a *finite* shear modulus on large scales.

Inspection of Fig. 2 shows that the data for  $\langle z \rangle$  exhibit a pronounced crossover from fluidlike behavior at large  $p$  to solidlike behavior at small  $p$ . More precisely, these data have the scaling form as given by (11) with  $\psi = \frac{1}{5}$ ,  $Z_{s0} \approx 1.5$ , and  $Z_{fl} \approx 0.5$ . These values may be used to construct the fluctuation-induced interaction

$$V_{FI}(l) \equiv T^2 / [c_1 \kappa l^2 + c_2 Y l^4], \quad (14)$$

with  $c_1 \approx 16$  and  $c_2 \approx 0.53$ . The asymptotic dependence of the membrane separation  $\langle l \rangle$  on pressure  $P$  can now be obtained by minimization of  $V_{FI}(l) + Pl$ .

In Figs. 1 and 2, we have also displayed the roughness  $\xi_{\perp}$  which should behave as  $\xi_{\perp} \sim \langle z \rangle$  for large  $\langle z \rangle$ . This is not obvious from Figs. 1 and 2 but it becomes evident in Fig. 3 where the ratio  $\xi_{\perp} / \langle z \rangle$  is shown as a function of  $1 / \langle z \rangle$ . Extrapolation to  $1 / \langle z \rangle = 0$  shows that this ratio has the finite limit  $\xi_{\perp} / \langle z \rangle \approx R_{s0} \approx 0.18 \pm 0.03$  for large  $\langle z \rangle$ . The solid line in Fig. 3 represents the ratio  $\xi_{\perp} / \langle z \rangle$  as obtained for fluid membranes with  $Y_0 = 0$ .<sup>14</sup> In this case,  $\xi_{\perp} / \langle z \rangle \approx R_{fl} \approx 0.41 \pm 0.01$ . Inspection of Fig. 3 also shows that the three sets of data corresponding to the last three rows in Table I indeed exhibit fluidlike behav-

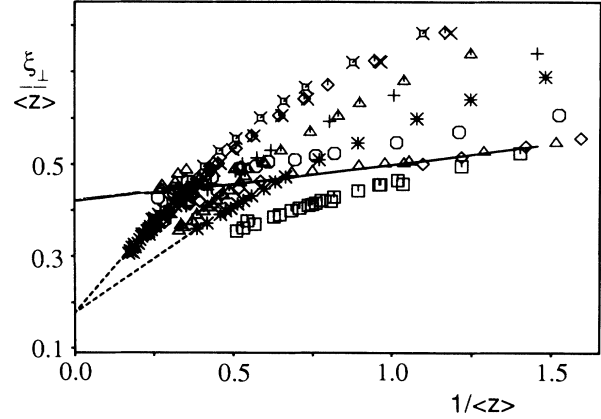


FIG. 3. Ratio  $\xi_{\perp} / \langle z \rangle$  as a function of  $1 / \langle z \rangle$ . The dashed line represents an extrapolation of the solidlike behavior while the solid line represents the fluidlike behavior. The symbols are explained in Table I.

ior over the accessible length scales.

Finally, let us consider the flickering of red blood cells, which has been experimentally studied for a long time.<sup>17,18</sup> The plasma membrane of these cells consists of a fluid lipid bilayer coupled to a network of rodlike spectrin molecules; it represents an example of a polymerized membrane provided the connectivity of the network does not change on experimentally relevant time scales. In the flicker experiments, one essentially measures the Fourier transform  $\bar{C}(q)$  of the correlation function  $\langle l(\mathbf{x}) l(\mathbf{0}) \rangle$ .<sup>18</sup> Our results imply that this function has the form

$$\bar{C}(q) = T / [c(TY)^{1/2} q^3 + \kappa q^4], \quad (15)$$

with  $c \approx 1.3$ . This implies the crossover length  $L^* \equiv 2\pi\kappa / c(TY)^{1/2}$ : The membrane is fluidlike and solidlike for wavelengths  $L < L^*$  and  $L > L^*$ , respectively.<sup>20</sup>

TABLE I. Values of elastic moduli used in the MC simulation; see Figs. 1-3. For comparison, the values for tethered networks (TNW) are also included.

$\kappa_0$	$K_{A0}$	$\mu_0$	$Y_0$	$z_0$	Symbol
0.0	0.6	0.4	0.96	0.0	⋈
0.001	0.6	0.4	0.96	0.032	◇
0.005	0.6	0.4	0.96	0.072	×
0.01	2.8	0.4	1.4	0.084	△
0.1	3.5	3.5	7.0	0.119	*
> 0.46			20	> 0.152	TNW
1.0	20.0	5.0	16.0	0.25	□
0.1	0.75	0.375	1.0	0.316	+
1.0	3.0	1.5	4.0	0.5	◇
0.5	0.75	0.375	1.0	0.707	○
1.0	0.75	0.375	1.0	1.0	△

For red blood cells, the elastic moduli of the plasma membrane are estimated to be<sup>18,21</sup>  $\kappa \approx 3 \times 10^{-20}$  J,  $K_A \approx 0.5$  J/m<sup>2</sup>, and  $\mu \approx 5 \times 10^{-6}$  J/m<sup>2</sup> which implies  $\Upsilon \approx 4\mu \approx 2 \times 10^{-5}$  J/m<sup>2</sup>. This would lead to  $L^* \approx 0.51$   $\mu\text{m}$  which is somewhat larger than the mesh size of the spectrin network. If one accepts this estimate for  $L^*$ , the experiments of Ref. 18 with  $L \gtrsim 0.5$   $\mu\text{m}$  have been limited to solidlike shape fluctuations. On the other hand, it should be possible to extend these measurements down to smaller values of  $L$  and thus to probe the full crossover towards the fluidlike shape fluctuations.

In summary, we have demonstrated (i) that polymerized or solidlike membranes are characterized by the roughness exponent  $\zeta = \frac{1}{2}$ , and (ii) that they can exhibit a crossover from fluidlike to solidlike behavior which should be observable, e.g., in experiments on red blood cells.

We acknowledge support by the Deutsche Forschungsgemeinschaft through Sonderforschungsbereich No. 266 and by Höchstleistungsrechenzentrum of the Forschungszentrum Jülich.

<sup>(a)</sup>New address: Institut für Festkörperforschung, Forschungszentrum Jülich, 5170 Jülich, Germany.

<sup>1</sup>See, e.g., E. Sackmann, P. Ettl, C. Fahn, H. Bader, H. Ringsdorf, and M. Schollmaier, *Ber. Bunsenges. Phys. Chem.* **89**, 1198 (1985); H. Gaub, B. Büschl, H. Ringsdorf, and E. Sackmann, *Chem. Phys. Lipids* **37**, 19 (1985).

<sup>2</sup>At low temperatures, lipid bilayers exhibit solidlike or crystalline phases denoted by  $L_\beta$  and  $L'_\beta$ . These solidlike membranes exhibit the same scaling properties as polymerized membranes provided one can suppress the proliferation of dislocations.

<sup>3</sup>See, e.g., Y. Kantor and D. R. Nelson, *Phys. Rev. Lett.* **58**, 2774 (1987).

<sup>4</sup>M. Plischke and D. Boal, *Phys. Rev. A* **38**, 4943 (1988).

<sup>5</sup>F. F. Abraham, W. E. Rudge, and M. Plischke, *Phys. Rev. Lett.* **62**, 1757 (1989).

<sup>6</sup>J.-S. Ho and A. Baumgärtner, *Phys. Rev. Lett.* **63**, 1324 (1989).

<sup>7</sup>D. R. Nelson and L. Peliti, *J. Phys. (Paris)* **48**, 1085 (1987).

<sup>8</sup>R. Lipowsky, *Europhys. Lett.* **7**, 255 (1988), and in *Random Fluctuations and Growth*, edited by H. E. Stanley and N. Ostrowsky (Kluwer, Dordrecht, 1988), p. 227. Unbinding transitions of polymerized membranes and the influence of a lateral tension  $\Sigma$  will be discussed elsewhere. If the bound state is induced by  $\Sigma$ , the membrane separation grows as  $1/\Sigma^{1/2}$  for small  $\Sigma$ .

<sup>9</sup>J. Aronowitz, L. Golubovic, and T. C. Lubensky, *J. Phys. (Paris)* **50**, 609 (1989).

<sup>10</sup>S. Leibler and A. Maggs, *Phys. Rev. Lett.* **63**, 406 (1989).

<sup>11</sup>J.-S. Ho and A. Baumgärtner, *Europhys. Lett.* **12**, 295 (1990).

<sup>12</sup>F. F. Abraham and D. R. Nelson, *Science* **249**, 393 (1990).

<sup>13</sup>L. D. Landau and E. M. Lifschitz, *Elastizitätstheorie* (Akademie-Verlag, Berlin, 1975).

<sup>14</sup>R. Lipowsky and B. Zielinska, *Phys. Rev. Lett.* **62**, 1572 (1989); R. Lipowsky and U. Seifert, in "Fluctuations in Lamellae and Membranes," edited by W. J. Benton and L. A. Turkevich (to be published).

<sup>15</sup>W. Helfrich, *Z. Naturforsch.* **33a**, 305 (1978).

<sup>16</sup>R. Lipowsky and S. Leibler, *Phys. Rev. Lett.* **56**, 2541 (1986).

<sup>17</sup>F. Brochard and J. F. Lennon, *J. Phys. (Paris)* **36**, 1035 (1975).

<sup>18</sup>A. Zilker, H. Engelhardt, and E. Sackmann, *J. Phys. (Paris)* **48**, 2139 (1987).

<sup>19</sup>The relaxation time  $t_R$  for a shape fluctuation of wavelength  $L$  grows as  $t_R \sim L^z$ , with  $z = 4 - \eta_\kappa = 2 + 2\zeta$ .

<sup>20</sup>Self-consistent perturbation theory for the effective bending rigidity implies the estimate  $c \approx 0.35$  as follows from the results of Y. Kantor and D. R. Nelson, *Phys. Rev. A* **36**, 4020 (1987).

<sup>21</sup>R. Waugh and E. A. Evans, *Biophys. J.* **26**, 115 (1979); H. Engelhardt and E. Sackmann, *Biophys. J.* **54**, 495 (1988).